PHYSICAL REVIEW B **76**, 205108 (2007)

Electronic structures of $Fe_{3-x}M_xO_4$ (M=Mn,Zn) spinel oxide thin films investigated by x-ray photoemission spectroscopy and x-ray magnetic circular dichroism

Junichi Takaobushi,[1] Mizue Ishikawa,[1] Shigenori Ueda,[2] Eiji Ikenaga,[3] Jung-Jin Kim,[3] Masaaki Kobata,[3] Yukiharu Takeda,[4] Yuji Saitoh,[4] Makina Yabashi,[3] Yoshinori Nishino,[5] Daigo Miwa,[5] Kenji Tamasaku,[5] Tetsuya Ishikawa,[5] Issei Satoh,[1] Hidekazu Tanaka,[1,*] Keisuke Kobayashi,[2] and Tomoji Kawai[1]
[1]*The Institute of Scientific and Industrial Research, Osaka University, 8-1 Mihogaoka, Ibaraki, Osaka 567-0047, Japan*
[2]*National Institute for Materials Science (NIMS), SPring-8, 1-1-1Kouto, Sayo-cho, Sayo-gun, Hyogo 679-5148, Japan*
[3]*JASRI, SPring-8, 1-1-1Kouto, Sayo-cho, Sayo-gun, Hyogo 679-5198, Japan*
[4]*JAEA, SPring-8, 1-1-1Kouto, Sayo-cho, Sayo-gun, Hyogo 679-5148, Japan*
[5]*RIKEN, SPring-8, 1-1-1Kouto, Sayo-cho, Sayo-gun, Hyogo 679-5148, Japan*

(Received 17 April 2007; published 15 November 2007)

We fabricated $Fe_{3-x}M_xO_4$ (M=Mn,Zn) thin film by pulsed laser deposition technique and investigated their electronic structure by hard x-ray photoemission spectroscopy (HX-PES) and x-ray magnetic circular dichroism (XMCD). HX-PES and XMCD revealed that the solid solution system of $Fe_{3-x}M_xO_4$ (M=Mn,Zn) is the best candidate for tunable ferromagnetic oxide semiconductor judging from systematic change of Fe, Mn core-level spectra, and valence band spectra by substitution. We present a model to explain modulation of electric and magnetic properties and electronic structure evolution caused by strongly correlated electron.

DOI: 10.1103/PhysRevB.76.205108 PACS number(s): 71.27.+a

INTRODUCTION

Spintronics devices are currently attracting much attention in the area of next-generation data storage, and the discovery of functional spintronics materials is quite important. The 3d transition metal oxides in strongly correlated electron systems[1] exhibit a rich variety of electrical and magnetic properties even at room temperature and are regarded as candidates for application in functional spintronics devices. For example, a tunneling magnetoresistance (TMR) effect near room temperature (RT) was reported for the $(La,Sr)MnO_3/SrTiO_3/(La,Sr)MnO_3$ junction[2] and Fe_3O_4 or $(NiFe_2O_4)/SrTiO_3/(La,Sr)MnO_3$ junction[3,4] utilizing their high-spin polarization. For further development of spintronics applications, the construction of advanced spin devices is indispensable and is not limited to TMR devices. Electric field control of ferromagnetism through carrier modulation is a typical example, as reported in the field-effect transistor (FET) structure using a dilute magnetic semiconductor of (In,Mn)As at 25 K.[5,6] In strongly correlated oxides, the control of ferromagnetism by an electric field is reported only in perovskite $(La,Ba)MnO_3/Pb(Zr,Ti)O_3$ FET[7] near RT utilizing carrier-mediated ferromagnetism. However, ferromagnetic FET devices using other oxides have not been reported. Fe-based oxides with spinel structures (spinel ferrite) exhibit ferrimagnetism with a very high Curie temperature (T_C) exceeding 800 K, which are used industrially for recoding media, and possess electric properties that are insulating. Only a few conductive spinel oxides [Fe_3O_4 (Ref. 8) and strained $NiFe_2O_4$ (Ref. 9)] are expected as half-metals and represent the most promising compounds for use as room-temperature TMR devices. These conducting spinel oxides have a huge carrier concentration ($\sim 10^{22}/cm^3$), which cannot be controlled by semiconductor technology. A tunable ferromagnetic semiconductor oxide with high T_C is required to realize oxide spintronics applications working at high temperature above RT.

EXPERIMENTAL DETAILS

The solid solution system of $Fe_{3-x}M_xO_4$ [M=Mn (Ref. 10) Zn (Ref. 11)] is possibly the best candidate in regard to tunability of carrier concentration, T_C, low-temperature fabrication, low cost, and environmental friendliness, as reported in our previous work.[10,11] In our experiment, we fabricated $Fe_{3-x}Mn_xO_4$ thin films (x=0, 0.1, 0.5, and 0.8) and $Fe_{3-x}Zn_xO_4$ thin films (x=0, 0.5, and 0.9) using a pulsed laser deposition (PLD) technique. Oxygen pressure (P_{O_2}) was set to 1.0×10^{-6} mbar, and the substrate temperature (T_s) was 320 °C during the deposition. Al_2O_3 (0001) single crystal (lattice mismatch of 8%) or MgO (100) single crystal (lattice mismatch of 0.3%) was used as a substrate. The crystal structure of films was determined using x-ray diffraction measurements. The Hall resistance measurements were performed at room temperature under a magnetic field from −9 to 9 T. Carrier concentration and carrier mobility of $Fe_{3-x}Mn_xO_4$ thin films (x=0, 0.1, 0.5, and 0.8) and $Fe_{3-x}Zn_xO_4$ thin films (x=0 and 0.5) were estimated from normal Hall components. The details are described in Refs. 10 and 11. Hard x-ray photoemission spectroscopy (HX-PES) was performed toward epitaxial $Fe_{3-x}Mn_xO_4$ thin films (x=0, 0.1, and 0.5) and $Fe_{3-x}Zn_xO_4$ thin films (x=0, 0.5, and 0.9) at SPring-8 (BL29XU and BL47XU, $h\nu$=7.94 keV at RT).[13] Total energy resolution was set to about 240 meV. The binding energy (E_B) was decided based on the Fermi level (E_F) of Au. X-ray absorption spectroscopy (XAS) measurements and x-ray magnetic circular dichroism (XMCD) were performed at SPring-8 (BL23SU in 3 T at 150 K). Film thickness was fixed to ~100 nm.

RESULTS AND DISCUSSIONS

Figure 1(a) shows the carrier concentration and mobility at 300 K of $Fe_{3-x}Mn_xO_4$ thin films (x=0, 0.1, 0.5, and 0.8) and $Fe_{3-x}Zn_xO_4$ thin films (x=0 and 0.5) prepared on MgO

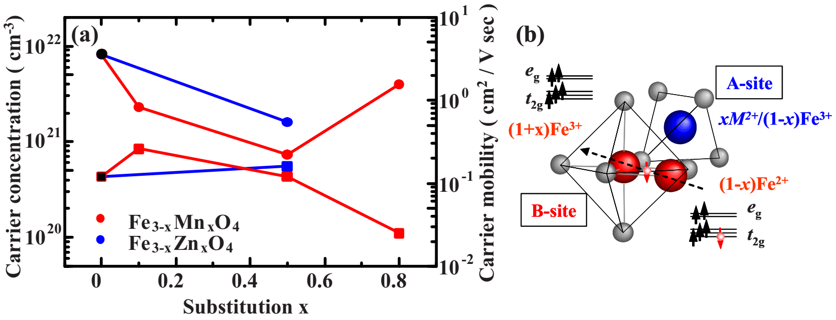

FIG. 1. (Color online) (a) Carrier concentration and carrier mobility of $Fe_{3-x}Mn_xO_4$ thin films ($x=0$, 0.1, 0.5, and 0.8) and $Fe_{3-x}Zn_xO_4$ thin films ($x=0$ and 0.5) with a substitution ratio estimated from an ordinary Hall resistance term (dR_{Hall}/dH at high magnetic field) (Refs. 10 and 11). (b) Schematic illustration of the carrier control mechanism in $Fe_{3-x}M_xO_4$ ($M=Mn,Zn$).

(001) single-crystal substrate using a PLD technique. The resistivities at 300 K of $Fe_{3-x}Mn_xO_4$ thin films ($x=0$, 0.1, and 0.5) (Ref. 10) and $Fe_{3-x}Zn_xO_4$ thin films ($x=0.5$ and 0.9) (Ref. 11) were 4.7×10^{-4}, 7×10^{-3}, 9×10^{-2}, 2.6×10^{-2}, and 2.8×10^{-1} Ω cm, respectively. The carrier concentration is systematically decreased, while the mobility is almost unchanged in the range $x=0-0.5$ for Mn and Zn substitutions. In detail, the original data (Hall effect against applied magnetic field in Ref. 10) clearly exhibit systematic increase of slope of normal Hall component, indicating systematic decrease of carrier concentration by Mn substitution. The large anomalous Hall effect in these systems indicates the presence of spin polarized carriers even above RT.[10,11] As for $x=0.9$, it was quite difficult to estimate Hall coefficient of $Fe_{2.1}Zn_{0.5}O_4$ thin film because high resistivity usually gives serious huge noise. In spite of these superior properties relative to present spintronics materials, their electronic structures have not been fully understood. In particular, details of the substitution effect on electrical transport properties remain unknown. In this work, we investigate epitaxial $Fe_{3-x}M_xO_4$ ($M=Mn,Zn$) thin films using HX-PES,[12] and propose a model for their spin and electronic structures. We conclude by discussing the construction of ferromagnetic spinel oxide-FET devices.

Figure 1(b) shows a schematic illustration of the ion configuration and spin structure for our proposed model to explain the physical properties of $Fe_{3-x}M_xO_4$ ($M=Mn,Zn$). The spinel-type Fe_3O_4 is the parent material and has two transition metal ion (Fe) positions at the A site surrounded by oxygen tetrahedra and at the B site surrounded by oxygen octahedra. Fe ions located at the A site are trivalent cations, and Fe ions at the B site are a mixed-valence state between trivalent and divalent cations.[14] The minority down-spin electron originated from the t_{2g} orbital of a high-spin Fe^{2+} at a B site and is considered a carrier hopping between Fe ions with spin polarization. There are ferromagnetic exchange interactions between B-B ions and strong antiferromagnetic exchange interactions between A-B ions, leading to high T_C (~860 K). If we selectively substitute a divalent cation for a trivalent cation at the A site, the carrier concentration decreases following a reduction of the Fe^{2+} ratio to maintain charge neutrality. This model explains the experimental results, as shown in Fig. 1(a). It is known that the Zn ion is completely substituted at the A site (normal spinel) in bulk $ZnFe_2O_4$,[15] and it is thought that the Mn ion is preferentially substituted at the A site in the case of bulk $MnFe_2O_4$.[16] We have already established formation condition of normal spinel $ZnFe_2O_4$ even in thin film.[18] We therefore believe that Zn or Mn substitution to Fe_3O_4 is suitable for controlling properties such as carrier concentration and magnetism.

Figure 2(a) shows Mn 2*p* core-level HX-PES spectra of $Fe_{3-x}Mn_xO_4$ thin films. Mn $2p_{3/2}$ peaks split into two peaks: a main peak at 640 eV and a satellite peak at 642 eV. The spectra are characteristically similar to the calculated spectra for atomic Mn^{2+}, and the satellite structure at 642 eV is of a very sharp form.[17] That is, the Mn ion in $Fe_{3-x}Mn_xO_4$ is a

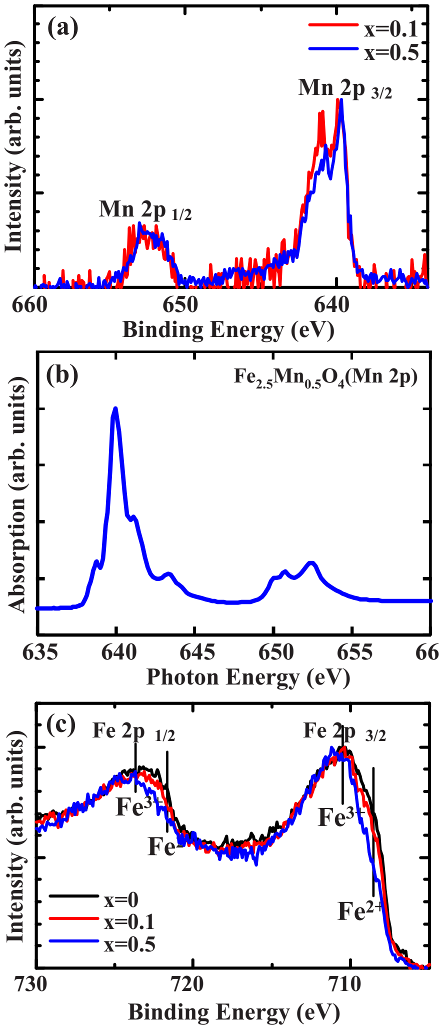

FIG. 2. (Color online) (a) Mn 2*p* core-level HX-PES spectra of $Fe_{3-x}Mn_xO_4$ thin films (0.1 and 0.5) taken at $h\nu=7.94$ keV. (b) Mn 2*p* core absorption spectrum of $Fe_{2.5}Mn_{0.5}O_4$ thin film under a magnetic field of 3 T at 150 K. (c) Fe 2*p* core-level HX-PES spectra of $Fe_{3-x}Mn_xO_4$ thin films (0, 0.1, and 0.5).

divalent cation and the electronic structure of the Mn^{2+} ion is localized with weak hybridization, indicating that Mn^{2+} has an ionic character at the A site. This result was confirmed by XAS measurements for Mn $2p$ core absorption of $\mathrm{Fe}_{2.5}\mathrm{Mn}_{0.5}\mathrm{O}_4$ thin film, as shown Fig. 2(b). The XAS calculations for Mn compound were reported in Ref. 19. The XAS spectrum is similar to the calculated Mn^{2+} (d^5) absorption spectra for a T_d symmetry rather than an O_h symmetry.[19] That is, The Mn $2p$ XAS spectra agree that Mn^{2+} ions are located in tetrahedral site rather than in octahedral site. It is thought that the Mn^{2+} ion is almost completely substituted at the A site. The unchanged mobility against Mn substitution also suggests that the Mn ion was substituted at the A site without disturbing the conducting path of the B site network.

Figure 2(c) shows Fe $2p$ core-level HX-PES spectra of $\mathrm{Fe}_{3-x}\mathrm{Mn}_x\mathrm{O}_4$ thin films. The energy positions of Fe^{2+} and Fe^{3+} components[20] are indicated by bars, as shown in Fig. 2(c). Fe^{2+} components decreased by substituting Mn^{2+} ions to $\mathrm{Fe}_3\mathrm{O}_4$. We believe that Fe^{2+} ions at the B site change to Fe^{3+} to maintain charge neutrality in the system by substituting Mn^{2+} ions to Fe^{3+} ions at the A site.

Figure 3(a) shows XMCD for Fe $2p$ core absorption. Figure 3(b) is the magnified figure in dashed area. We normalized the XMCD signal, in Fig. 3, by XMCD intensity at photon energy of 714 eV to keep the background. (The peak energy position for each Fe ion was obtained from Ref. 20. In more detail, current opinions of relationship between the cation valencies and photoemission or XMCD of magnetite are, for example, revised in Ref. 21. Our labeling of the photoemission and XMCD lines based on Ref. 20 well explained the tendency both on the change of electronic structure and physical properties against x with good consistency.) To evaluate ratio of Fe ion located at each site more accurately, we added following figure of XMCD intensities for $(\mathrm{Fe}^{2+})_\mathrm{B}$, $(\mathrm{Fe}^{3+})_\mathrm{B}$, $(\mathrm{Fe}^{2+})_\mathrm{A}$ normalized by that for $x=0$ component as Fig. 3(c). The XMCD signal of Fe^{3+} at the B site increased, while those of Fe^{2+} at the B site and Fe^{3+} at the A site decreased with increasing Mn^{2+} concentration (x). This result indicates that Fe^{3+} at the B site increased with increasing x, while Fe^{2+} at the B site and Fe^{3+} at the A site decreased by Mn^{2+} substitution, respectively. In addition, HX-PES spectra and XAS spectra indicated that Mn^{2+} is located at tetrahedral A site. Therefore, it is concluded that at the effect of $[\mathrm{Mn}^{2+}]_\mathrm{A}$ ions ($x=0-0.5$) involved an increase in the valency of Fe ions at the B site, which resulted in the maintenance of charge neutrality. That is, following formula (1) shows the results obtained by HX-PES or XMCD.

$$[\mathrm{Fe}^{3+}(\downarrow:5\mu_B)_{1-x}\mathrm{Mn}^{2+}(\downarrow:5\mu_B)_x]_\mathrm{A}\mathrm{O} \times[\mathrm{Fe}^{3+}(\uparrow:5\mu_B)_{1+x}\mathrm{Fe}^{2+}(\uparrow:4\mu_B)_{1-x}]_\mathrm{B}\mathrm{O}_3. \qquad (1)$$

Furthermore, the conducting carrier path among Fe ions at the B site is not disturbed because Mn is substituted at the A site. Thus, the proposed model shown in Fig. 1(b) successfully explains the reduction of carrier concentration and unchanged mobility in the range $x=0-0.5$ (Ref. 22) for $(\mathrm{Fe}_{3-x}\mathrm{Mn}_x)\mathrm{O}_4$, as seen in Fig. 1(a).

Bulk $\mathrm{ZnFe}_2\mathrm{O}_4$ has a normal spinel structure.[15] Experiments with $\mathrm{Fe}_{3-x}\mathrm{Zn}_x\mathrm{O}_4$ thin film show that the lattice constant increases proportionally with increasing Zn concentration. That is, the change of lattice constant follows Vegard's law.[11] Figure 1(a) shows that the carrier mobility is constant, suggesting that the $\mathrm{Fe}_{3-x}\mathrm{Zn}_x\mathrm{O}_4$ film adopts a normal spinel structure. Thus, Zn ions in $\mathrm{Fe}_{3-x}\mathrm{Zn}_x\mathrm{O}_4$ thin films are divalent cations and are located at the A site.

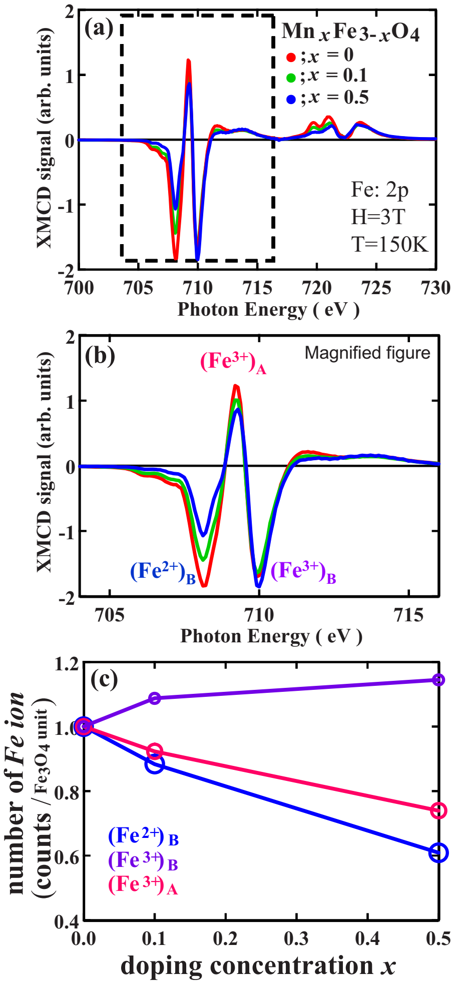

FIG. 3. (Color online) (a) Mn substitution ratio (x) dependence of x-ray magnetic circular dichroism (XMCD) spectra for $(\mathrm{Fe}_{3-x}\mathrm{Mn}_x)\mathrm{O}_4$ thin films ($x=0$, 0.1, and 0.5) obtained from the intensity difference between core absorption spectra taken at opposite helicity. (b) The magnified figure in dashed area. The peak energy position for each Fe ion was obtained from Ref. 20 (c) Mn substitution ratio (x) dependence of XMCD spectra for $(\mathrm{Fe}^{2+})_\mathrm{B}$, $(\mathrm{Fe}^{3+})_\mathrm{B}$, and $(\mathrm{Fe}^{2+})_\mathrm{A}$ normalized by that for $x=0$ component.

The characteristic evolutions in electronic structure of $\mathrm{Fe}_{3-x}\mathrm{Mn}_x\mathrm{O}_4$ were observed clearly in the normal spinel $\mathrm{Fe}_{3-x}\mathrm{Zn}_x\mathrm{O}_4$ system. Figure 4 shows Fe $2p$ core-level HX-PES spectra of $\mathrm{Fe}_{3-x}\mathrm{Zn}_x\mathrm{O}_4$ thin films. As with $\mathrm{Fe}_{3-x}\mathrm{Mn}_x\mathrm{O}_4$ thin films, the intensity of Fe^{2+} components at the $E_B=709$ and 723 eV decreased by substituting Zn^{2+}.[20] To maintain charge neutrality by substituting Zn^{2+} to Fe^{3+} at the A site, the Fe^{2+} component at the B site decreases in accordance with the following formula:

$$[\mathrm{Fe}^{3+}(\downarrow:5\mu_B)_{1-x}\mathrm{Zn}^{2+}{}_x]_\mathrm{A}\mathrm{O} \times[\mathrm{Fe}^{3+}(\uparrow:5\mu_B)_{1+x}\mathrm{Fe}^{2+}(\uparrow:4\mu_B)_{1-x}]_\mathrm{B}\mathrm{O}_3. \qquad (2)$$

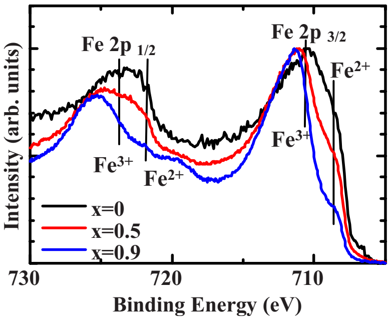

FIG. 4. (Color online) Fe $2p$ core-level HX-PES spectra of $Fe_{3-x}Zn_xO_4$ thin films (0, 0.5, and 0.9) taken at $h\nu=7.94$ keV.

According to the proposed model, shown in Fig. 1(b), we can expect the density of states (DOS) at the E_F to decrease with increasing substitution of both Mn and Zn. Figure 5 shows electronic structures of valence band HX-PES spectra near E_F for $Fe_{2.5}Mn_{0.5}O_4$ thin film, $Fe_{3-x}Zn_xO_4$ thin films ($x=0.5$ and 0.9), Fe_3O_4 thin film ($x=0$), and bulk $ZnFe_2O_4$ ($x=1.0$ in $Fe_{3-x}Zn_xO_4$). DOS near E_F is systematically decreased by substituting Mn or Zn. The important feature in the valence band spectra is the decrease of the peak intensity around 0.5 eV, as indicated by arrows in Fig. 5. The peak around 0.5 eV corresponds to a minority down-spin electron state that originated from the Fe t_{2g} orbital at the B site. This electron corresponds to the carriers according to the band calculation of Anisimov *et al.*[23] We see that changes in peak intensity correspond to the reduction of carrier concentration in Fig. 1(a). This change in valence band spectra explains the modulation of electrical properties by the substitution. The decrease in carrier concentration mainly originated from the reduction of the down-spin state in the t_{2g} orbital of the mixed-valence state of $[Fe]_B$ ions by substituting Mn^{2+} or Zn^{2+} at the A site.

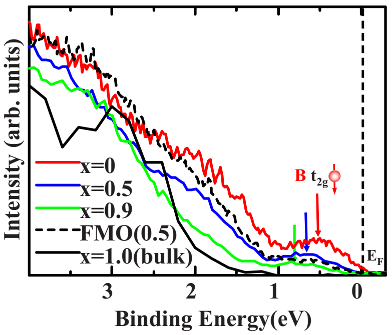

FIG. 5. (Color online) Valence band HX-PES spectra of $Fe_{2.5}Mn_{0.5}O_4$ thin film, $Fe_{3-x}Zn_xO_4$ thin films (0, 0.5, and 0.9), and bulk $ZnFe_2O_4$ taken at $h\nu=7.94$ keV.

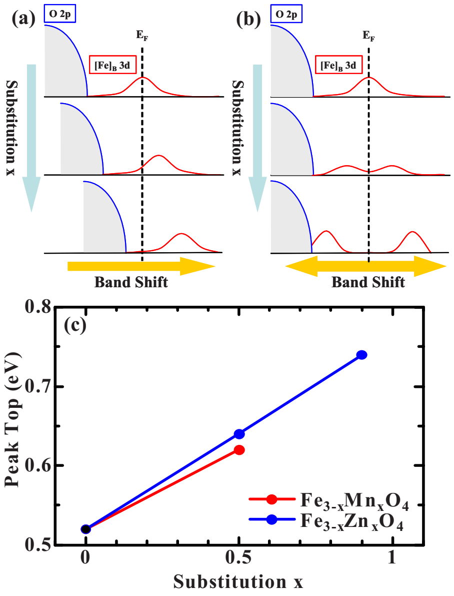

FIG. 6. (Color online) Schematic illustration of electronic structure evolution by M^{2+} substitution. (a) Rigid band model. (b) Mott-Hubbard model. Only O $2p$ and Fe $3d$ at the B site are shown for simplicity. DOS of Fe and M^{2+} ions at the A site were omitted. (c) Dependence of 0.5 eV peak position on Mn and Zn substitutions for $Fe_{3-x}Mn_xO_4$ thin films ($x=0$ and 0.5) and $Fe_{3-x}Zn_xO_4$ thin films ($x=0$, 0.5, and 0.9).

The peak shift in Fig. 5 suggests the importance of electron correlation effects in this material. If the $Fe_{3-x}M_xO_4$ ($M=Mn,Zn$) system is a conventional semiconductor, decreasing the carrier concentration only causes a chemical potential shift on the basis of the rigid band model, as shown in Fig. 6(a), and all peaks should shift to the lower E_B side in the case of electron reduction. However, experimental results showed that the peak near 0.5 eV of $Fe_{3-x}Zn_xO_4$ (t_{2g}) shifted to the higher E_B side with an increasing Zn ratio, a response that was also seen in $Fe_{3-x}Mn_xO_4$ with $x=0.5$. Furthermore, core-level spectra for Mn $2p$, Zn $3d$, Fe $2p$, O $2p$, and O $1s$ did not shift against E_F. Figure 6(c) plots the peak shift of the t_{2g} down-spin state of $Fe_{3-x}M_xO_4$ ($M=Mn,Zn$) thin films. The energy difference of the peak position is 250 meV between $x=0$ and 0.9. We analyzed this phenomenon using another model because it cannot be explained by a rigid band model. The Mott-Hubbard model, shown in Fig. 6(b), may be used to explain the spectral change as follows: (i) the Fe^{2+} ratio to Fe^{3+} at the B site decreases by substituting Zn^{2+}, (ii) the electron-electron correlation (effective Coulomb interaction) increases with decreasing screening effect due to the reduction of carrier concentration, (iii) consequently, the gap becomes larger and the peak shifts to the higher E_B side, and finally, (iv) the Mott gap is formed at the $x=1$ component ($ZnFe_2O_4$). The band shift toward the higher E_B side in Fig. 5 is attributed to the Mott-Hubbard model. This means that $Fe_{3-x}M_xO_4$ ($M=Mn,Zn$) thin films have wide tunability in the concentration of their spin polarized carriers by adjusting the electron-electron correlation. That is, $Fe_{3-x}M_xO_4$ ($M=Mn,Zn$) thin films are considered magnetic semiconductors[10,11] with a strong electron correlation in the wide substitution range.

We believe that this strong electron correlation plays an important role in switching devices using carrier-induced phase transition such as a Mott-FET.[24] Here, we discuss the strength of the electron-electron correlation (U_{eff}/t) of the spinel Fe oxide system in the context of the Mott-Hubbard model, where U_{eff} and t are the effective Coulomb interaction and transfer integral between d electrons, respectively.

The electronic structure of $Fe_{3-x}M_xO_4$ (M=Mn,Zn) evolutes as a Mott-Hubbard type, as shown in Fig. 6(b). The U_{eff} for the d^5 high-spin configuration is larger than that for other d-electron configurations in $3d$ transition metal ions.[25] Heavily substituted $Fe_{3-x}M_xO_4$ (M=Mn,Zn) has an electron configuration similar to that of d^5 (Fe^{3+}) with a high-spin state. In addition, t of the t_{2g} band (corresponding to the conduction band of spinel Fe oxides) is smaller than that of the e_g band. Therefore, U_{eff}/t is quite larger in $(Fe_{3-x}Mn^{2+}{}_x)O_4$ and $(Fe_{3-x}Zn^{2+}{}_x)O_4$ than in other $3d$ metal oxides, such as ferromagnetic perovskite manganite (d^4 system with e_g conduction band) and high T_C superconductive cuprate (d^9 system with e_g conduction band),[26] and the effective Mott gap then prevents the appearance of a metallic phase except near the x=0 substitution region. The electrical transport properties of $Fe_{3-x}M_xO_4$ (M=Mn,Zn) are mainly tuned by modulating the effective Coulomb interaction without an accompanying chemical shift as recorded for a typical magnetic semiconductor with a strongly correlated electron system. The reduced and highly correlated carriers in $Fe_{3-x}M_xO_4$ are superior to those of perovskite manganite and superconductive cuprate and will help to realize a Mott metal-insulator transition using semiconductor technology.

CONCLUSIONS

In conclusion, we prepared $Fe_{3-x}M_xO_4$ (M=Mn,Zn) thin films and measured their electronic structure using HX-PES. Core-level spectra of the $Fe_{3-x}M_xO_4$ (M=Mn,Zn) films showed that Mn and Zn ions were substituted with a divalent cation at the A site, and Fe^{2+} components decreased with substitution of Mn and Zn. Valence band spectra revealed that DOS near E_F of $Fe_{3-x}M_xO_4$ (M=Mn,Zn) thin films systematically decreased with increasing Mn and Zn concentrations. The band shift for changing electron correlation was observed in a wide substitution range. This band shift is interpreted by the change of U_{eff}/t on the basis of a Mott-Hubbard model. The $Fe_{3-x}M_xO_4$ (M=Mn,Zn) system is a typical magnetic semiconductor with a strong electron correlation. The findings of this investigation suggest that this material system holds great promise for the development of advanced spin electronics, especially for devices working at high temperature.

ACKNOWLEDGMENTS

The authors acknowledge A. Fujimori (University of Tokyo) for x-ray magnetic circular dichroism measurements, and M. Kanai, T. Yanagida (Osaka University), A. Kimura, and A. Tanaka (Hiroshima University) for helpful discussions. This work was partially supported by the Ministry of Education, Science, Sports and Culture through the Center of Excellence (COE) program, a Grant-in-Aid for Scientific Research (B) (No. 16360007), and SENTAN, JST.

---

*h-tanaka@sanken.osaka-u.ac.jp

[1] C. H. Ahn, A. Bhattacharya, M. Di Ventra, J. N. Eckstein, C. Daniel Frisbie, M. E. Gershenson, A. M. Goldman, I. H. Inoue, J. Mannhart, A. J. Millis, A. F. Morpurgo, D. Natelson, and J.-M. Triscone, Rev. Mod. Phys. **78**, 1185 (2006).

[2] Y. Lu, X. W. Li, G. Q. Gong, G. Xiao, A. Gupta, P. Lecoeur, J. Z. Sun, Y. Y. Wang, and V. P. Dravid, Phys. Rev. B **54**, R8357 (1996).

[3] X. W. Li, A. Gupta, G. Xiao, W. Qian, and V. P. Dravid, Appl. Phys. Lett. **73**, 3282 (1998).

[4] U. Lüders, M. Bibes, K. Bouzehouane, E. Jacquet, J.-P. Contour, S. Fusil, J.-F. Bobo, J. Fontcuberta, A. Barthélémy, and A. Fert, Appl. Phys. Lett. **88**, 082505 (2006).

[5] H. Ohno, D. Chiba, F. Matsukura, T. Omiya, E. Abe, T. Dietl, Y. Ohno, and K. Ohtani, Nature (London) **408**, 944 (2000).

[6] D. Chiba, M. Yamanouchi, F. Matsukura, and H. Ohno, Science **301**, 943 (2003).

[7] T. Kanki, Y.-G. Park, H. Tanaka, and T. Kawai, Appl. Phys. Lett. **83**, 4860 (2003).

[8] Y. S. Dedkov, U. Rüdiger, and G. Güntherodt, Phys. Rev. B **65**, 064417 (2002).

[9] U. Lüders, M. Bibes, J.-F. Bobo, M. Cantoni, R. Bertacco, and J. Fontcuberta, Phys. Rev. B **71**, 134419 (2005).

[10] M. Ishikawa, H. Tanaka, and T. Kawai, Appl. Phys. Lett. **86**, 222504 (2005).

[11] J. Takaobushi, H. Tanaka, and T. Kawai, S. Ueda, J.-J. Kim, M. Kobata, E. Ikenaga, M. Yabashi, K. Kobayashi, Y. Nishino, D. Miwa, K. Tamasaku, and T. Ishikawa, Appl. Phys. Lett. **89**, 242507 (2006).

[12] K. Kobayashi, M. Yabashi, Y. Takata, T. Tokushima, and S. Shin, K. Tamasaku, D. Miwa, T. Ishikawa, H. Nohira, T. Hattori, Y. Sugita, O. Nakatsuka, A. Sakai, and S. Zaima, Appl. Phys. Lett. **83**, 1005 (2003).

[13] H. Tanaka, Y. Takata, K. Horiba, M. Taguchi, A. Chainani, S. Shin, D. Miwa, K. Tamasaku, Y. Nishino, T. Ishikawa, E. Ikenaga, M. Awaji, A. Takeuchi, T. Kawai, and K. Kobayashi, Phys. Rev. B **73**, 094403 (2006).

[14] Z. Zhang and S. Satpathy, Phys. Rev. B **44**, 13319 (1991).

[15] J. M. Hastings and L. M. Corliss, Rev. Mod. Phys. **25**, 114 (1953).

[16] J. M. Hastings and L. M. Corliss, Phys. Rev. **104**, 328 (1956).

[17] Y. Yamamoto, H. Tanaka, and T. Kawai, Jpn. J. Appl. Phys., Part 2 **40**, L545 (2001).

[18] P. Wernet, B. Sonntag, M. Martins, P. Glatzel, B. Obst, and P. Zimmermann, Phys. Rev. A **63**, 050702(R) (2001).

[19] G van der Laan and I. W. Kirkman, J. Phys.: Condens. Matter **4**, 4189 (1992).

[20] Y. X. Lu, J. S. Claydon, Y. B. Xu, S. M. Thompson, K. Wilson, and G. van der Laan, Phys. Rev. B **70**, 233304 (2004).

[21] J. García and G. Subías, J. Phys.: Condens. Matter **16**, R145 (2004).

[22] The mobility of $Fe_{3-x}Mn_xO_4$ with x=0.8 suddenly decreased by 1 order of magnitude. For this reason, it is thought that the Mn ion partially occupied the B site and disturbed the conducting path in the heavy substitution region.

[23] V. I. Anisimov, I. S. Elfimov, N. Hamada, and K. Terakura, Phys.

Rev. B **54**, 4387 (1996).

[24] D. M. Newns, J. A. Misewich, C. C. Tsuei, A. Gupta, B. A. Scott, and A. Schrott, Appl. Phys. Lett. **73**, 780 (1998).

[25] M. Imada, A. Fujimori, and Y. Tokura, Rev. Mod. Phys. **70**, 1039 (1998).

[26] M. Taguchi, A. Chainani, K. Horiba, Y. Takata, M. Yabashi, K. Tamasaku, Y. Nishino, D. Miwa, T. Ishikawa, T. Takeuchi, K. Yamamoto, M. Matsunami, S. Shin, T. Yokoya, E. Ikenaga, K. Kobayashi, T. Mochiku, K. Hirata, J. Hori, K. Ishii, F. Nakamura, and T. Suzuki, Phys. Rev. Lett. **95**, 177002 (2005).